The FMN-Binding Domain of Cytochrome P450BM-3: Resolution, Reconstitution, and Flavin Analogue Substitution†

Donovan C. Haines, Irina F. Sevrioukova,‡ and Julian A. Peterson*

Department of Biochemistry, The University of Texas Southwestern Medical Center at Dallas, Dallas, Texas 75390-9038

Received February 3, 2000; Revised Manuscript Received May 25, 2000

ABSTRACT: Cytochrome P450BM-3 is a self-sufficient bacterial protein containing three naturally fused domains which bind either heme, FMN, or FAD. Resolution of protein and FMN from the isolated FMN-containing domain of cytochrome P450BM-3 was accomplished using trichloroacetic acid. The apoprotein thus prepared was shown to rebind FMN to regenerate the original holoprotein as indicated by both spectroscopy and activity measurements. To better understand how the protein/flavin interaction might contribute to reactivity, the association process was studied in detail. Fluorescence quenching was used to measure a dissociation constant of the flavin−protein complex of 31 nM, comparable to FMN-containing proteins of similar reactivity and higher than that of flavodoxins. Stopped-flow kinetics were performed, and a multistep binding process was indicated, with an initial k_{on} value of 1.72×10^5 M^{-1} s^{-1}. Preparation of the apoprotein allowed substitution of flavin analogues for the native FMN cofactor using 8-chloro-FMN and 8-amino-FMN. Both were found to bind efficiently to the protein with only minor variations in affinity. Reductive titrations established that, as in the native FMN-containing FMN-binding domain, the 8-amino-FMN-substituted domain does not produce a stable one-electron-reduced species during titration with sodium dithionite. The 8-chloro-FMN-substituted domain, however, had sufficiently altered redox properties to form a stable red anionic semiquinone. The 8-chloro-FMN-substituted FMN-binding domain was shown in reconstituted systems to retain most of the cytochrome *c* reductase activity of the native domain but only a very small amount of palmitic acid hydroxylase activity. The 8-amino-FMN-substituted FMN-binding domain showed no palmitic acid hydroxylase activity and only 30% of the native cytochrome *c* reductase activity, demonstrating the importance of thermodynamics to the mechanism of this protein.

Cytochrome P450BM-3,[1] a fatty acid monooxygenase from *Bacillus megaterium*, resembles eukaryotic P450s in primary structure and function (*1*, *2*). This self-sufficient enzyme is a complex, multidomain protein containing heme, FAD, and FMN bound to a single polypeptide chain (*1*). The functional domains of P450BM-3, containing either the heme (the heme domain, BMP), both flavins (the reductase domain, BMR), the FMN (the FMN-binding domain), the FAD (the FAD-binding domain), or both the heme and FMN (BMP/FMN-binding domain), were separately cloned and expressed in bacteria (*3*−*9*). The solubility and ease of high-level expression of the holoenzyme and its functional domains make this protein a very attractive model for studying mammalian P450s.

The FAD/FMN-containing reductase domain of P450BM-3 shows 33% identity with mammalian NADPH−cytochrome P450 reductase (CPR) with highly conserved regions involved in the binding of the flavins and pyridine nucleotide (*2*). The NADPH/FAD- and FMN-binding domains of both reductases were proposed to be related to ferredoxin $NADP^+$ reductase (FNR) and flavodoxins, respectively (*10*, *11*). Strong experimental evidence in support of this hypothesis was provided when the flavin domains of CPR and BMR were separately expressed in *E. coli* (*6*, *7*, *12*, *13*), and later when the X-ray crystal structure of rat liver CPR was determined (*14*, *15*). Besides the FNR- and flavodoxin-like domains, CPR was found to have an α-helical domain connecting the two flavin domains, and it was concluded that this domain was responsible for maintaining both the distance between the flavins and their relative orientation (*15*).

Studies on electron donor−acceptor properties of BMR and kinetics of reduction of the flavins in BMR and in the holoenzyme of P450BM-3 by NADPH (*16*, *17*) have revealed that the reductase domain of P450BM-3, despite being functionally analogous to CPR, adopted a different mechanistic strategy to control the redox potential and electron flow between the flavins and from the flavins to

† This work was supported in part by Grant R01-GM50858 from the NIH.

* Address correspondence to this author. Email: Julian.Peterson@email.swmed.edu. Phone: 214-648-2361. Fax: 214-648-8856.

‡ Present address: Department of Molecular Biology and Biochemistry, University of California, Irvine, CA 92697-3900.

[1] Abbreviations: FMN, flavin adenine mononucleotide; FAD, flavin adenine dinucleotide; MOPS, morpholinopropane-*O*-sulfonic acid; P450BM-3, CYP102 isolated from *Bacillus megaterium*; BMP, the 55-kDa heme domain of P450BM-3; BMR, the 66-kDa FMN/FAD-binding domain of P450BM-3; BMP/FMN-binding domain, the naturally fused heme- and FMN-binding domains of P450BM-3; FMN-binding domain, the 20-kDa FMN-containing domain of P450BM-3; apo-FMN-binding domain, the apoprotein of the FMN-binding domain; FAD-binding domain, the 46-kDa NADPH- and FAD-binding domain of P450BM-3; FNR, ferredoxin $NADP^+$ reductase; CPR, mammalian NADPH−cytochrome P450 reductase; 8-Cl-FMN, 8-chloro-FMN; 8-NH_2-FMN, 8-amino-FMN; 8-Cl-FAD, 8-chloro-FAD; 8-NH_2-FAD, 8-amino-FAD; TCA, trichloroacetic acid; TLC, thin-layer chromatography.

10.1021/bi000255p CCC: $19.00
Published on Web 07/11/2000

the heme of the P450. The FMN moiety was found to be mainly responsible for the unusual redox properties of BMR (*6, 16, 17*). The midpoint reduction potentials of BMR involving FMN appeared to be considerably more positive than those for FAD, while the midpoint reduction potential for the FMN semiquinone/$FMNH_2$ couple was more positive than that for FMN/FMN semiquinone. Only the low-potential anionic FMN semiquinone form of BMR was shown to be capable of reducing the heme iron in P450BM-3, whereas the two-electron-reduced form of FMN, being thermodynamically more stable, was unreactive in electron transfer to the heme. In contrast, CPR transfers electrons to P450 by shuttling between hydroquinone and semiquinone forms of the FMN, delivering one electron per cycle (*18, 19*).

The expression of the separate FMN-binding domain of P450BM-3 (*6, 7*) allowed large quantities of this protein to be obtained for structural and mechanistic studies. Some of its features have been characterized (*6, 8*). The flavin in the FMN-binding domain was shown to retain the redox and electron-accepting properties of BMR-bound FMN (*6*). The fact that cytochrome *c* reductase and palmitic acid hydroxylase activities of intact P450BM-3 could be partially reconstituted in the reaction mixture consisting of separate heme, FAD, and FMN domains (*6, 8*) indicates that the FMN-binding domain is capable of accepting and transferring electrons from the FAD-binding domain to cytochrome *c* or BMP, respectively.

Recently, the crystal structure of a putative electron-transfer complex between the heme domain of P450BM-3 and the FMN-binding domain was solved, allowing a more detailed analysis of both the structure of the FMN-binding domain and its interaction with the heme domain (*20*). The asymmetric unit of the crystal included two heme domains and one FMN-binding domain, with the linker between the heme and FMN-binding domains absent due to proteolysis. Only one heme domain was in direct contact with the FMN-binding domain. In this structure, the edge of the FMN cofactor is exposed on the surface of the FMN-binding domain at the interface to the complexed heme domain. In fact, Q387 from a peptide loop of the heme domain (the "meander") passes within 4 Å of the methyl edge of the flavin cofactor in the FMN-binding domain, with the heme iron 18.4 Å away from the FMN through space. Although providing an interesting picture of the interaction of the methyl edge of the FMN cofactor with the heme domain, the structure still leaves many questions unanswered. For example, the structure of the highly homologous CPR is mutually exclusive with this complex, as the methyl edge of CPR's FMN-binding domain is in contact with the FAD methyl edge of CPR's FAD-binding domain (*15*). The FAD-binding domain occupies the same space as the P450BM-3 heme domain in the complex structure. It seems unlikely that two systems that are so highly genetically and functionally homologous have evolved different dynamic mechanisms or electron-transfer pathways.

To obtain further insights into the structure/function relationships in the FMN-binding domain of P450BM-3, we have undertaken the study of the properties of the apo-FMN-binding domain and its interaction with FMN, FMN analogues, FAD, and riboflavin. In the present study, the reversible dissociation of the FMN-binding domain into apoprotein and flavin was achieved using trichloroacetic acid as a denaturing agent. Of the natural flavins, the apo-FMN-binding domain appeared to bind FMN specifically. We report some of the redox and electron-accepting and -transferring properties of 8-Cl-FMN- and 8-NH_2-FMN-substituted FMN-binding domain. Both of the flavin analogue-substituted FMN-binding domains were found to be capable of accepting electrons from the FAD-binding domain and reducing cytochrome *c*, but not BMP, in the reconstitution system consisting of the three separate domains of P450BM-3 (*8*).

MATERIALS AND METHODS

Materials. 8-Cl-FAD and 8-NH_2-FAD were kindly provided by Dr. Vincent Massey (The University of Michigan, Ann Arbor, MI). FAD, riboflavin, phosphodiesterase (*Naja naja* snake venom), cytochrome *c*, and NADPH were from Sigma (St. Louis, MO). Sodium dithionite was obtained from Hardman and Holden, Ltd. (Manchester, England). All other reagents were of the purest grade available.

General Methods. UV−visible spectroscopy was performed on either a Hewlett-Packard Model 8452A Diode Array Spectrophotometer or a Varian Cary 100 double beam instrument. Protein concentrations were estimated (*21*) using bovine serum albumin as a standard. The heme-, FMN-, and FAD-binding domains of P450BM-3 were purified as previously described (*6, 9*). The concentration of BMP was determined by the method of Omura and Sato (*22*) using $\Delta\epsilon_{448nm} = 91\ mM^{-1}\ cm^{-1}$. The concentrations of the FMN- and FAD-binding domains were determined spectrophotometrically, using $\epsilon_{466nm} = 9.8\ mM^{-1}\ cm^{-1}$ and $\epsilon_{452nm} = 10.4\ mM^{-1}\ cm^{-1}$, respectively. The concentration of free FMN in the solution was measured spectrophotometrically using $\epsilon_{445nm} = 12.2\ mM^{-1}\ cm^{-1}$ (*23*).

8-Cl- and 8-NH_2-FMN were prepared by the enzymatic hydrolysis of 8-Cl-FAD ($\epsilon_{448nm} = 10.6\ mM^{-1}\ cm^{-1}$) and 8-$NH_2$-FAD ($\epsilon_{482nm} = 44.0\ mM^{-1}\ cm^{-1}$), respectively. The 0.1 mM FAD analogues in 100 mM phosphate buffer, pH 7.0, were incubated for 4 h in the dark at room temperature with phosphodiesterase (*Naja naja* snake venom, 1 mg/mL). The proteins were separated from the flavins by ultrafiltration of the samples in Centricon-3 concentrators (Amicon).

Preparation of the Apo-FMN-Binding Domain. Apoprotein of the FMN-binding domain of P450BM-3 was prepared as described previously for flavodoxins (*24*) with minor variations. Cold trichloroacetic acid (TCA) was mixed with a 0.5 mM solution of the FMN-binding domain in 100 mM phosphate buffer, pH 7.0, and 0.3 mM EDTA (buffer A) at 4 °C to give a final concentration of 5% (w/v) TCA. After 5 min in darkness, the mixture was centrifuged (10000*g* for 10 min). The precipitate was dissolved in buffer A, and the procedure described above was repeated 1 more time. The final precipitate was dissolved in a minimal volume of buffer A and dialyzed overnight against the same buffer to remove traces of TCA. Apoprotein was stored at 4 °C for short-term storage or at −80 °C for long-term storage. The apoprotein was incubated in the presence of 10 mM β-mercaptoethanol before use to obtain optimal binding of flavin, presumably due to formation of intermolecular disulfide bonds via oxidation of the domain's lone cysteine residue.

Spectrophotometric Titrations. Spectrophotometric titrations of FMN, FMN analogues, riboflavin, and FAD with apoprotein of the FMN-binding domain were carried out in a 2 mL cuvette in buffer A at room temperature. Following the addition of aliquots of apoprotein, the reaction mixture was permitted to stand until no further absorbance change occurred. The concentration of apoprotein was measured spectrophotometrically by titration into a known amount of FMN, or using the dye-binding assay of Bradford (*25*) with the native FMN-binding domain as a standard.

Fluorescence Titrations. Values for the K_d's of the complex of the apo-FMN-binding domain with flavins were determined by fluorescence titrations performed with either a Photon Technology International fluorometer or a Perkin-Elmer LS-50B luminescence spectrophotometer in a cuvette of 1 cm light path at room temperature with $\lambda_{ex} = 450$ nm and $\lambda_{em} = 525$ nm from FMN and 8-Cl-FMN, and $\lambda_{ex} = 478$ nm and $\lambda_{em} = 525$ nm for 8-NH_2-FMN. The standard assay mixture contained 1 μM flavin, 100 mM phosphate buffer, pH 7.0, 0.3 mM EDTA. Apoprotein was added in increments to the FMN solution, and the fluorescence was noted after each addition. The use of a 185 μM apoprotein stock solution ensured that no titration was diluted more than 2−3%. The titration was continued until additions of apoprotein caused no further decreases in flavin fluorescence. K_d values were calculated by correcting the fluorescence data for dilution and fitting the data to the equation: $y = fl_\infty + (fl_0 - fl_\infty) \times (1 - [FMN]/[FMN]_0)$ where fl_∞ is the fluorescence at the end of the titration (well beyond the equivalence point), fl_0 is the fluorescence before the addition of any apoprotein, and $[FMN]_0$ is 1×10^{-6} M. [FMN] is the positive root of the quadratic equation $x^2 - (p_0 + [FMN]_0 + K_d) \times x + ([FMN]_0 + p_0) = 0$ and is a function of p_0 (the total concentration of filled and unfilled binding sites, i.e., the total protein added) and the fit parameter K_d. Small errors in protein concentration cause least-squares routines to compensate for an altered end point by changing the K_d, rendering the value obtained useless and preventing the attainment of a good fit by most any measure. To avoid this, the value of p_0 was calculated using the concentration of protein stock as a second fitting parameter, and the value obtained was always verified to ensure it did not deviate more than 20% from the expected protein concentration. For the analogues, the p_0 found for that batch of protein was fixed, and $[FMN]_0$ was a fitted parameter. These equations describe the solution to a model that assumes there exists a single binding site that is 0% occupied at fl_0 fluorescence and 100% occupied at fl_∞ fluorescence, and find a best value for K_d and the concentration of active sites in the stock solution.

Reductive Titrations. Anaerobic spectrophotometric titrations of 8-Cl- and 8-NH_2-FMN-substituted FMN-binding domain with sodium dithionite were performed in 100 mM phosphate buffer, pH 7.0, as previously described for the native FMN-binding domain (*6*).

Enzymatic Activity Assays. The cytochrome *c* reductase activity was measured in the reaction mixture consisting of 20 nM FAD-binding domain, 200 nM FMN-binding domain or flavin analogue-substituted FMN-binding domain, and 100 μM cytochrome *c* in 50 mM MOPS buffer, pH 7.5, at 30 °C. The reaction was initiated by the addition of NADPH (100 μM final concentration). Specific activity was calculated employing $\epsilon_{550nm} = 21$ mM^{-1} cm^{-1}.

The palmitic acid hydroxylase activity was determined using the reconstitution system consisting of the three separate domains of P450BM-3. The reaction mixture contained 60 nM BMP, 0.6 μM FMN or flavin analogue-substituted FMN-binding domain, 1.8 μM FAD-binding domain, and 100 μM palmitic acid in 50 mM MOPS buffer, pH 7.5. The reaction was initiated by the addition of 200 μM NADPH and carried out at 25 °C. The preparation of the radioactive substrate, extraction, TLC separation, and quantification of the products of the reaction were performed as described elsewhere (*8*).

Stopped-Flow Kinetics. All stopped-flow fluorescence experiments were carried out on a Bio-Logic (Grenoble, France) SFM3 mixer using a quartz suprasil TC-100/10F cuvette with path lengths of 1.0 cm and 1.0 mm parallel and perpendicular to the excitation beam, respectively. Experiments were kept at 25 °C by use of a circulating water bath connected to the SFM3's water jacket. Syringes were computer-controlled using Bio-Logic's MPS software.

For monitoring of fluorescence, a Bio-Logic HgXe modular light source and excitation monochromator set to 450 nm were coupled to the SFM-3 through fiber-optic cables. Fluorescence was detected with the supplied PMS-400 photomultiplier system utilizing an Oriel #52101 low fluorescence long-pass filter (Oriel, Stratford, CT) to select for fluorescence emission over 500 nm; 180 μL each of 1 μM apo-FMN-binding domain and 5−30 μM FMN, both in 100 mM potassium phosphate buffer, pH 7.0, 0.3 mM EDTA, was mixed over 30 ms and the fluorescence monitored for 60 s. Data were collected every 5 ms from 0 ms to 2 s and every 100 ms thereafter using Bio-Logic's BioKine software.

For monitoring absorbance, a Bio-Logic Xe modular light source with the excitation monochromator set for 0 nm (white light) was coupled to the SFM-3 through fiber-optic cables. Transmitted light was detected with a J&M Tidas16 512 diode array detector for multiwavelength data collection (Molecular Kinetics, Pullman, WA) coupled to the SFM3 through fiber-optic cables. For each trace, 180 μL of 22 μM apo-FMN-binding domain and 180 μL of 20 μM FMN, both in 100 mM potassium phosphate buffer, 0.3 mM EDTA, pH 7.0, were mixed over 30 ms, and the UV−visible spectrum was monitored for 60 s. Data were collected from 200 to 740 nm with 2 nm resolution. The system allows variation of the data collection frequency over the course of the experiment. A spectrum was taken initially every 5 ms, every 100 ms from 300 ms to 10 s, and every 1.00 s thereafter.

Raw data were exported to Sigma Plot 3.0 (Jandel Scientific) via ASCII files. Stopped-flow data (UV−vis or fluorescence quenching) were time-corrected by subtracting the mixing time (30 ms) and adding the dead time (2.3 ms) of the instrument under experimental conditions. Fluorescence progress curves were fit first (without weighting) by the single-exponential equation: $y = a_1 + a_2 \times t + a_3 \times \exp(a_4 \times t)$, where a_n indicates a fit parameter; then by the double exponential equation: $y = a_1 + a_2 \times t + a_3 \times \exp(a_4 \times t) + a_5 \times \exp(a_6 \times t)$. Experiments in which enzyme-free buffer was mixed with FMN indicated a slight ($\sim 5 \times 10^{-4}$ V/s) linear decrease in fluorescence with time, thus the requirement of the linear ($a_2 \times t$) term. In UV−vis experiments, no such decrease was observed, so progress curves

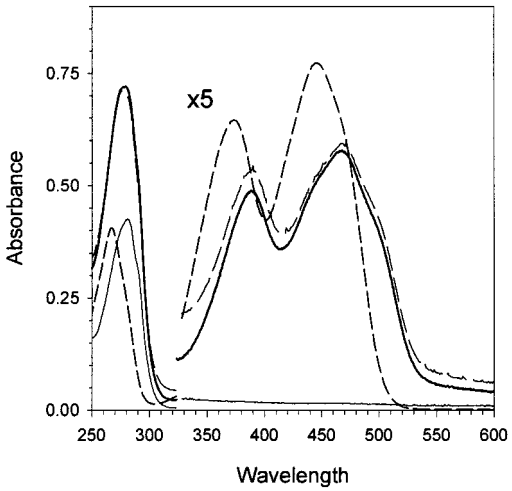

FIGURE 1: Absorption spectra of the apoprotein, native, and FMN-reconstituted FMN-binding domain of P450BM-3, and free FMN. Spectra of 7.5 μM apoprotein (—), 16 μM native FMN-binding domain (– –), 14 μM FMN-reconstituted FMN-binding domain (thick solid line), and 12 μM FMN (- - -) were recorded in 100 mM phosphate buffer, pH 7.0, with 0.3 mM EDTA.

were fit to the corresponding single-exponential equation: $y = a_1 + a_2 \times \exp(a_3 \times t)$, where a_n indicates a fit parameter; then by the double exponential equation: $y = a_1 + a_2 \times \exp(a_3 \times t) + a_4 \times \exp(a_5 \times t)$.

RESULTS

Removal of FMN from the FMN-Binding Domain of P450BM-3. A striking characteristic of the FMN-binding domain of P450BM-3 is its high thermostability. To release the flavin from the protein by heating, samples had to be boiled for at least 20−30 min. During that period of time, the solution changed from yellow−green to bright yellow, indicating that the flavin had dissociated from the protein. The absence of a pellet upon centrifugation indicated that heating did not irreversibly aggregate the protein. Moreover, the color of the solution gradually returned to yellow−greenish, indicating the formation of the FMN-bound protein. If the boiling time was shorter than 20 min, the FMN was found to rebind to the apoprotein immediately upon cooling.

In the present study, to prepare the apoprotein of the FMN-binding domain of P450BM-3, we used TCA, a strong denaturing agent, for precipitation of the apoprotein according to the method of Wassink and Mayhew (*24*), as described under Materials and Methods. The procedure allowed the removal of FMN reversibly from the FMN-binding domain and gave high yields of active apoprotein (>90%). As seen in Figure 1, the absorbance spectrum of the apoprotein of the FMN-binding domain has a maximum at 280 nm with $\epsilon_{280nm} = 34 \pm 4$ mM^{-1} cm^{-1}, and no traces of the flavin are present in the preparation.

Binding of Flavins by Apoprotein of the FMN-Binding Domain of P450BM-3. In common with many other flavoproteins, the visible absorbance spectrum of the FMN-binding domain of P450BM-3 differs from that of free FMN (Figure 1). The absorbance maxima of free FMN are at 372 and 448 nm, whereas those for the FMN-binding domain are significantly shifted to longer wavelengths and are located at 388 and 468 nm. Figure 2 shows the absorbance spectral changes observed during the spectrophotometric titration of free FMN with apoprotein. The dramatic spectral changes at 358, 440, and 502 nm, isosbestic points at 330, 385, 410, and 470 nm, and the appearance of a long-wavelength absorbance band occurring upon binding of the flavin to the apoprotein are noticeable (Figure 2A). The absorbance changes at 502 nm reached a maximum after addition of approximately 1.5 mol of apoprotein per mole of FMN (Figure 2B). The intercept around 1.0 indicates that there is only one FMN-binding site in the FMN-binding domain molecule. The spectra of reconstituted and native FMN-binding domain are identical (Figure 1).

In addition to binding FMN, the apo-FMN-binding domain was found to form complexes with FMN analogues. The spectral changes observed during titrations of 8-Cl-FMN and 8-NH_2-FMN with apoprotein are shown in Figure 3 and Figure 4, respectively. Binding of 8-Cl-FMN by the apo-FMN-binding domain was similar to that of FMN and resulted in the appearance of isosbestic points at 378 and 462 nm, a decrease and shift of the absorbance maxima of free flavin from 360 and 448 nm to 384 and 466 nm in 8-Cl-

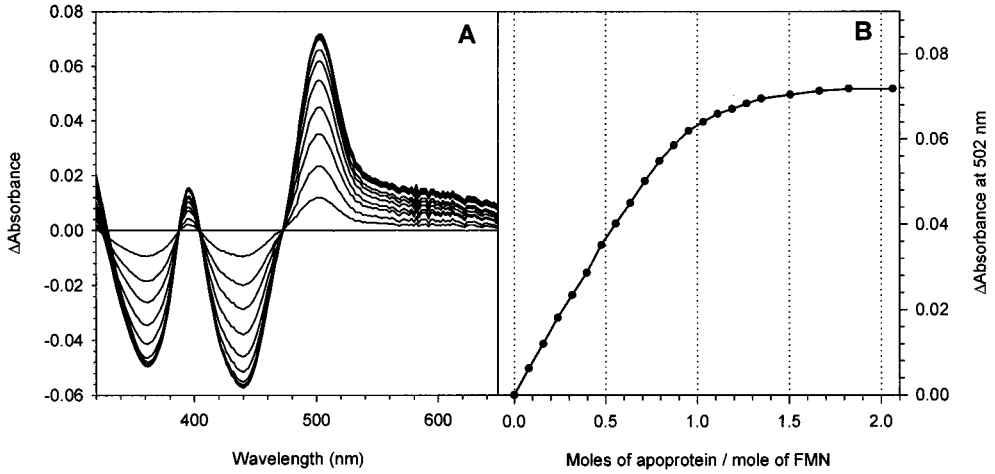

FIGURE 2: Spectrophotometric titration of FMN with the apo-FMN-binding domain of P450BM-3. (A) Absorbance spectral changes on FMN binding to apoprotein. 15 μM FMN in 100 mM phosphate buffer, pH 7.0, 0.3 mM EDTA was titrated with 200 μM apoprotein of the FMN-binding domain. Difference spectra were recorded after each addition of titrant. (B) The number of binding sites for FMN was determined from the change of absorbance at 502 nm caused by binding of FMN to the apoprotein.

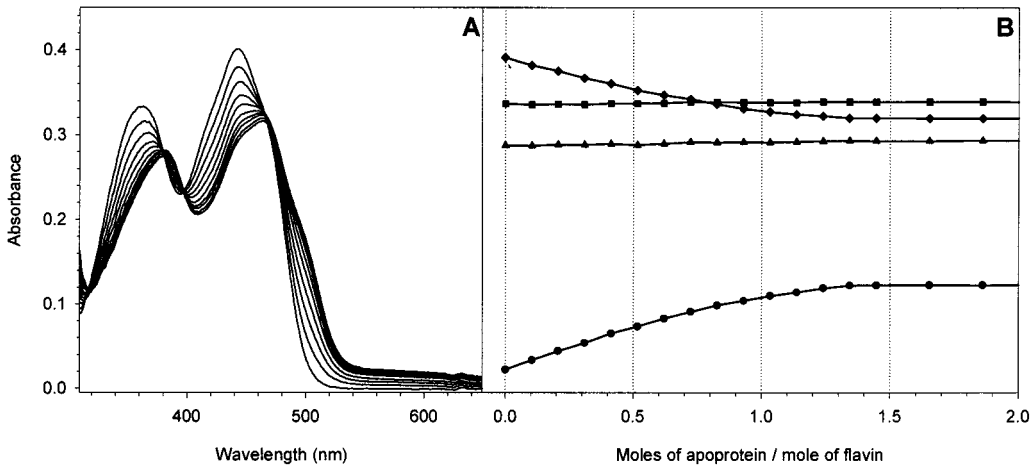

FIGURE 3: Spectrophotometric titration of 8-Cl-FMN with the apo-FMN-binding domain of P450BM-3. (A) 40 μM 8-Cl-FMN in 100 mM phosphate buffer, pH 7.0, 0.3 mM EDTA was titrated with 400 μM apo-FMN-binding domain. Spectra were recorded after each addition of titrant. (B) Plot of absorbance changes at 378 nm (▲), 444 nm (◆), 462 nm (■), and 510 nm (●) as a function of apoprotein added.

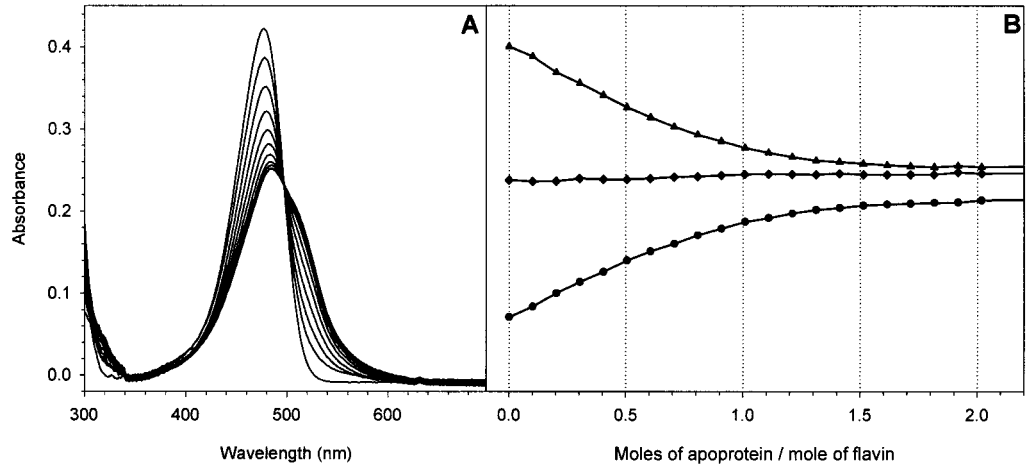

FIGURE 4: Spectrophotometric titration of 8-NH_2-FMN with the apo-FMN-binding domain of P450BM-3. (A) 13 μM 8-NH_2-FMN in 100 mM phosphate buffer, pH 7.0, 0.3 mM EDTA was titrated with 200 μM apo-FMN-binding domain. Spectra were recorded after each addition of titrant. (B) Plot of absorbance changes at 478 nm (▲), 496 nm (◆), and 510 nm (●) as a function of apoprotein added.

FMN-bound FMN-binding domain, and an increase in the absorbance near 500 nm and in the long-wavelength region. The extinction coefficient for the 8-Cl-FMN-substituted FMN-binding domain at 466 nm was found to be 9.6 ± 0.2 mM^{-1} cm^{-1}.

Conversion of 8-NH_2-FMN from the free to the FMN-binding domain-bound form caused a significant absorbance decrease around 480 nm, and the appearance of a pronounced shoulder at 510 nm and an isosbestic point at 496 nm (Figure 4). The spectrum of the 8-NH_2-FMN-substituted FMN-binding domain has one maximum at 486 nm with an extinction coefficient of 33.0 ± 3.0 mM^{-1} cm^{-1}. The color of the solution upon flavin binding changed from yellow to salmon pink.

An absence of absorbance changes after addition of the apoprotein to either riboflavin or FAD (data not shown) suggests that the apoprotein of the FMN-binding domain does not efficiently bind these flavins.

Fluorescence intensity changes were measured in order to estimate the K_d of the complexes of FMN and flavin analogues with the apo-FMN-binding domain. When apoprotein was added to FMN, the fluorescence decrease was nearly linear with apo-FMN-binding domain added over most of the titration curve, indicating the complex is strong. The residual fluorescence in the presence of excess apoprotein was 3−4%. The average value of K_d, calculated from values determined by application of nonlinear regression to five such titrations, was found to be 31 ± 8 nM. It should be mentioned that the fluorescence excitation and emission spectra of the reconstituted FMN-binding domain were similar to those for the native protein.

The K_ds for the dissociation of the flavin analogues from the analogue-substituted FMN-binding domains were estimated similarly. As with FMN, when apoprotein was added to the analogue, the fluorescence decrease was nearly linear with the apo-FMN-binding domain added over most of the titration curve, indicating the binding is tight. The traces obtained for fluorescence quenching of FMN analogues were very similar to those for FMN; all three flavins bind with similar affinity. Values of the K_d of 117 ± 24 and 23 ± 9 nM for 8-Cl-FMN and 8-NH_2-FMN were obtained, respectively.

Stopped-Flow Studies of Flavin Binding. To gain insight into the mechanism of flavin binding to apoprotein of the FMN-binding domain, stopped-flow fluorescence studies were performed. Upon binding, partial quenching of fluorescence emitted at 525 nm when FMN was excited at 450 nm was observed, as can be seen in the typical trace shown

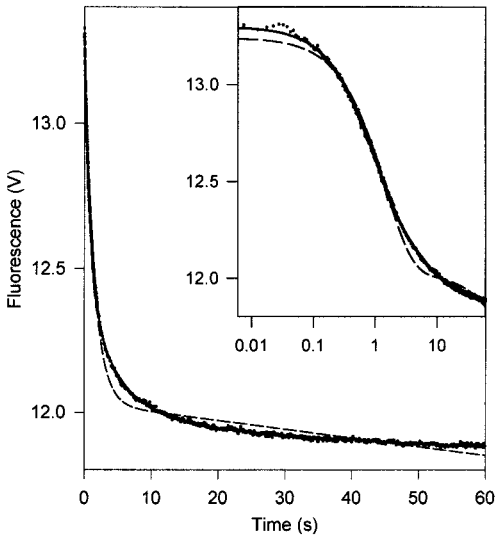

FIGURE 5: Typical stopped-flow fluorescence progress curve for flavin binding. Equal volumes of 1 μM apo-FMN-binding domain and 10 μM FMN, both in 100 mM potassium phosphate buffer, 0.3 mM EDTA, pH 7.0, were mixed, and >500 nm fluorescence emission from 450 nm excitation was monitored with time as described under Materials and Methods. The inset is identical to the major graph except that the time axis is displayed logarithmically for examination of the early phase of the reaction. The premixing portion has been removed, and time scales have been adjusted by subtracting the mixing time (30 ms) and adding the dead time (2.3 ms). (●) Experimental data; (- - -) nonlinear least-squares best fit of the single exponential equation: $y = a_1 + a_2 \times t + a_3 \times \exp(a_4 \times t)$ where a_n indicates fitting parameters found to be 12.03 V, -3.05×10^{-3} V s^{-1}, 1.21 V, and 0.69 s^{-1} for a_1, a_2, a_3, and a_4, respectively; (—) nonlinear least-squares best fit of the double exponential equation: $y = a_1 + a_2 \times t + a_3 \times \exp(a_4 \times t) + a_5 \times \exp(a_6 \times t)$ where a_n indicates fitting parameters found to be 11.96 V, -1.43×10^{-3}, 0.88 V, 1.16 s^{-1}, 0.46 V, and 0.19 s^{-1} for a_1, a_2, a_3, a_4, a_5, and a_6, respectively.

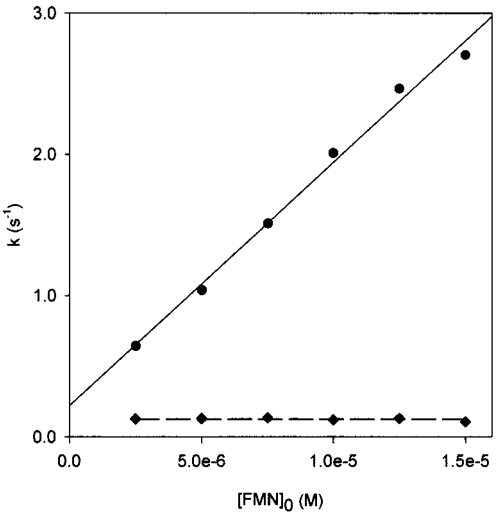

FIGURE 6: Concentration dependence of stopped-flow fluorescence relaxation times. Individual fluorescence quenching traces were fit to the two exponential equation: $y = a_1 + a_2 \times t + a_3 \times \exp(a_4 \times t) + a_5 \times \exp(a_6 \times t)$, where a_n indicates a fit parameter, as described under Materials and Methods. The kinetic parameters a_4 and a_6 are plotted against the initial concentration of free FMN (half of the concentration of the mixing solution). (●) a_4 data point; (◆) a_6 data point; (—) linear least-squares fit of a_4 data (slope = 1.72×10^5 M^{-1} s^{-1}, intercept = 0.220 s^{-1}, $r^2 = 0.993$); (— —) average value of a_6 data (data were not concentration-dependent; see text), 0.1246 s^{-1}.

in Figure 5. As this figure clearly shows, the data could not be fit properly by an equation describing a single exponential decay (see Materials and Methods), but required a double exponential decay indicating either a multistep process or multiple forms of apo-FMN-binding domain are present in solution. To assist in distinguishing between these two possibilities, a study of the dependence of the relaxation times on the concentration of FMN under conditions of large excess of FMN was undertaken. It was found that although the faster, larger decay showed a very linear dependence upon FMN concentration as seen in Figure 6 the slower, weaker decay seemed to be independent of the FMN concentration. Experimental limits on the determination of the slower relaxation time cause some uncertainty in this conclusion.

Although there are other possibilities, a model for such two-exponential data in flavodoxins has been proposed with two equilibria present (*26*). First, free flavin and free apoprotein are in equilibrium with a form of 'loosely' reconstituted protein. This form of reconstituted protein then relaxes in a second equilibrium to a more tightly complexed form according to the following scheme:

$$E + F \underset{k_{-1}}{\overset{k_1}{\rightleftharpoons}} EF_1 \underset{k_{-2}}{\overset{k_2}{\rightleftharpoons}} EF_2$$

In analyzing the two relaxation times obtained, results such as those in Figure 6 with a fast step of linear dependence and a slow step of hyperbolic (in this case, the linear portion of the hyperbola) indicate that a slow equilibrium is preceded by a fast one. In such a case, the slope of the line for the faster relaxation gives k_1 (*26*). The intercept of that line is given by $k_{-1} + k_2 + k_{-2}$. If the second curve is fully determined, its intercept on the *y*-axis yields k_{-2}, and the asymptote gives $k_2 + k_{-2}$, allowing calculation of k_{-2} and thereby k_{-1}. Unfortunately, the data for the second relaxation are not adequate for full analysis due to the very small fluorescence change associated with this relaxation, and it seems unlikely that significantly better data can be collected at this time. What can be determined is that the second relaxation appears constant over the concentrations tested, and the average value obtained (corresponding to $k_2 + k_{-2}$) is 0.125 s^{-1}. This yields a k_{-1} of 0.095 s^{-1} from the intercept of the linear trace, making the true dissociation constant of the first step 552 nM since the k_1 value was determined from the slope of the linear trace to be 1.72×10^5 M^{-1} s^{-1}. Since this is much larger than the overall effective dissociation constant, $k_2 \gg k_{-2}$, so k_2 will be slightly less than 0.125 s^{-1}. The end result is $k_1 = 1.72 \times 10^5$ M^{-1} s^{-1}, $k_{-1} = 0.095$ s^{-1}, $k_2 \approx 0.125$ s^{-1}, and $k_{-2} \ll 0.125$ s^{-1}.

Identification of a multistep binding equilibrium during the binding of FMN by the apo-FMN-binding domain is made difficult by the low amplitude of the slower transition's fluorescence quenching and the tendency for stopped-flow methods to contain slight deviations from theory due to artifacts. In addition, it is possible small amounts of altered forms of the apoprotein could be present that bind flavin at different rates than the major form. Verification that this slower transition is not such an artifact comes from a comparison of the predicted K_d values and the concentration dependence of the relaxations. Static titrations, as mentioned previously, yielded a K_d of 30 nM. Applying a single-step model to the concentration-dependent stopped-flow data, however, predicts a K_d in the micromolar range. The

discrepancy is too large to result from possible small deviations in experimental conditions, and would indicate a second equilibrium exists even if the second transition had not been observed in the traces at all. The lack of a dependence of the rate of the slower relaxation on the flavin concentration (over the range of concentrations studied) indicates that the slower, low-amplitude relaxation cannot be due to the presence of a small amount of a tighter binding form of apoprotein.

Although the second step in the binding mechanism could not be well enough resolved to determine specific rate constants, it is interesting to examine the sum of the rate constants, which was determined. The sum of the kinetic constants determined for the second equilibrium step of flavin binding agrees quite well with values determined for a flavodoxin from *A. vinelandii*. In this flavodoxin, k_1, k_{-1}, k_2, and k_{-2} were determined to be 5.3×10^4 M^{-1} s^{-1}, 8.1×10^{-3} s^{-1}, 0.16 s^{-1}, and 4.2×10^{-3} s^{-1}, respectively (*26*). The kinetic constants for the second equilibrium in *A. vinelandii* match very well those found for the FMN-binding domain of P450BM-3, where $k_2 + k_{-2} = 0.125$ s^{-1} with $k_2 \gg k_{-2}$ as required in P450BM-3 to get a static dissociation constant (K_d^{app}) much lower than the intrinsic dissociation constant (K_d^1).

A stopped-flow experiment monitoring the entire UV−visible spectrum was performed in an attempt to verify the existence of the intermediate in the multistep binding mechanism and to verify that the second relaxation is not merely an artifact of the fluorescence technique. The use of a diode-array detector allowed the collection of a three-dimensional data set, taking the entire spectrum from 200 to 740 nm with 2 nm resolution at a high sampling frequency (see Materials and Methods). Figure 7 shows the change in absorbance at several important wavelengths with time. Although at no wavelength was a clear maxima obtained indicative of an intermediate, the data shown again fit a double exponential equation much better than a single exponential.

Anaerobic Titrations of Reconstituted FMN-Binding Domain with Sodium Dithionite. During anaerobic titrations of the FMN-reconstituted FMN-binding domain of P450BM-3 with sodium dithionite (data not shown), absorbance changes were identical to those for the native protein (*6*), indicating that the redox properties of the protein-bound FMN were not perturbed after denaturation and reconstitution of the holoprotein.

The reduction of the 8-Cl-FMN-substituted FMN-binding domain with sodium dithionite was somewhat different (Figure 8). Addition of up to 0.5 mol of the reductant per mole of protein caused partial bleaching of the absorbance at 466 nm and formation of a spectral species with an absorbance maximum at 382 nm, characteristic of a red, anionic flavin semiquinone (Figure 8A,C). An isosbestic point at 524 nm was observed during this phase. Further titrations by sodium dithionite caused no further changes in the visible spectrum. It should be noted that the equilibrium in the reaction mixture after each addition of the reductant was established extremely slowly. It takes 2 days to complete the reduction of the 8-Cl-FMN-substituted FMN-binding domain. The fact that the stoichiometry between the amount of sodium dithionite added and the protein was greater than

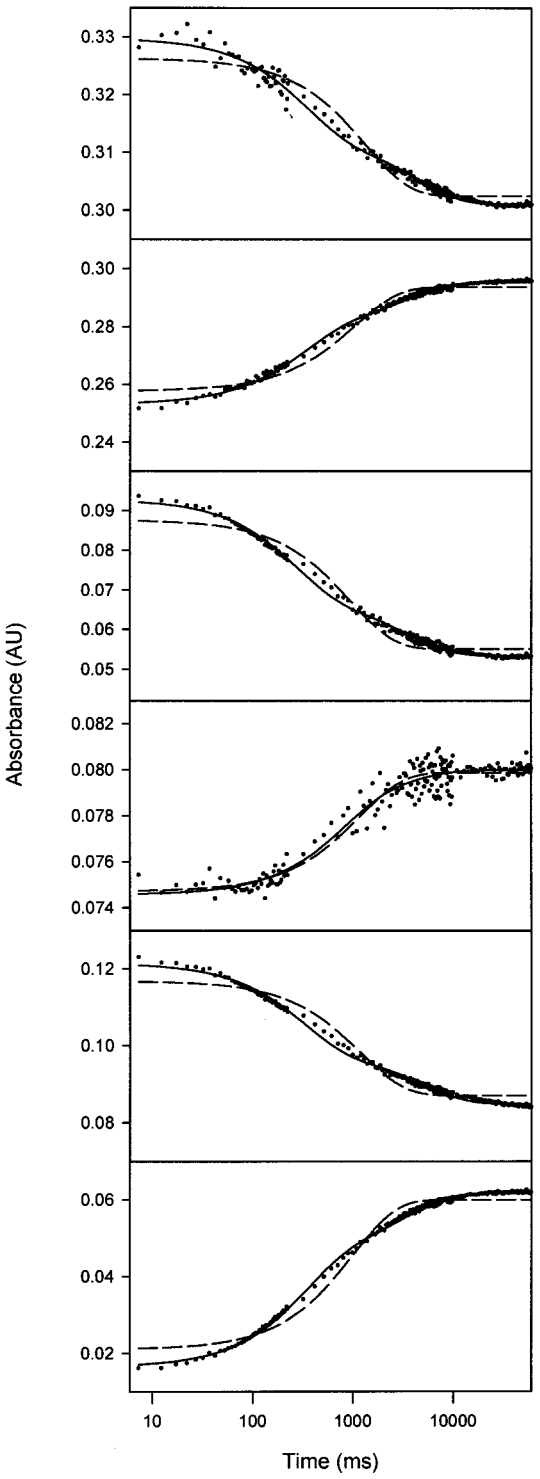

FIGURE 7: Stopped-flow UV−vis progress curves. Partial representation of the three-dimensional dataset obtained when equal volumes of 22 μM apo-FMN-binding domain and 20 μM FMN, both in 100 mM potassium phosphate buffer, 0.3 mM EDTA, pH 7.0, were mixed and the UV−visible spectrum was monitored via a diode array detection system as described under Materials and Methods. From top to bottom, traces represent the time course at 264, 292, 358, 396, 440, and 502 nm. For each trace, the premixing portion has been removed, and the time scale has been adjusted by subtracting the mixing time (30 ms) and adding the dead time (2.3 ms). (●) Experimental data; (− −) best fit of the single exponential equation: $y = a_1 + a_2 \times \exp(a_3 \times t)$ where a_n indicates a fit parameter; (−) best fit of the double exponential equation: $y = a_1 + a_2 \times \exp(a_3 \times t) + a_4 \times \exp(a_5 \times t)$ where a_n indicates a fit parameter.

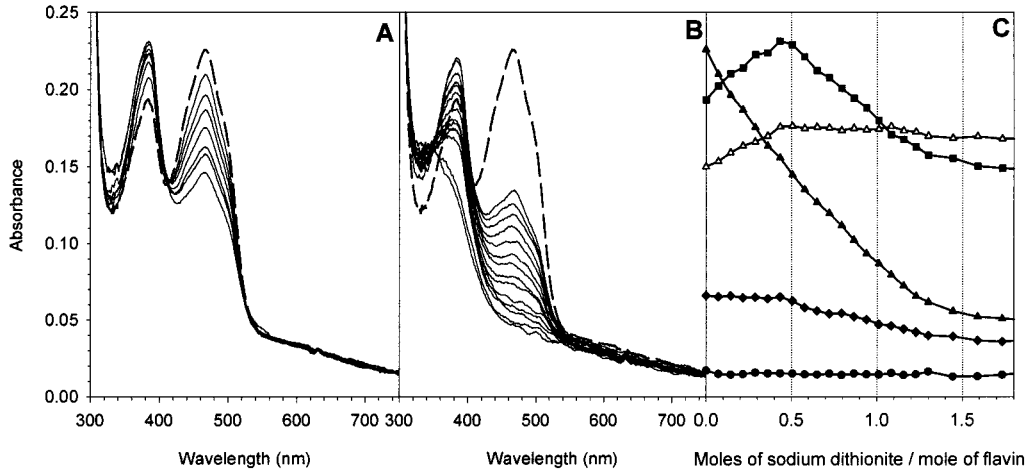

FIGURE 8: Anaerobic titration of the oxidized 8-Cl-FMN-substituted FMN-binding domain of P450BM-3 with sodium dithionite. The 8-Cl-FMN-substituted FMN-binding domain (24 μM) in 100 mM phosphate buffer, pH 7.0, was titrated with sodium dithionite (2 mM). Panels A and B represent a single titration of the protein. Sets of curves are separated in the figure to show isosbestic points occurring during the titration. Panel C is a plot of absorbance changes at 355 nm (△), 392 nm (■), 466 nm (▲), 524 nm (◆), and 750 nm (●) as a function of apoprotein added.

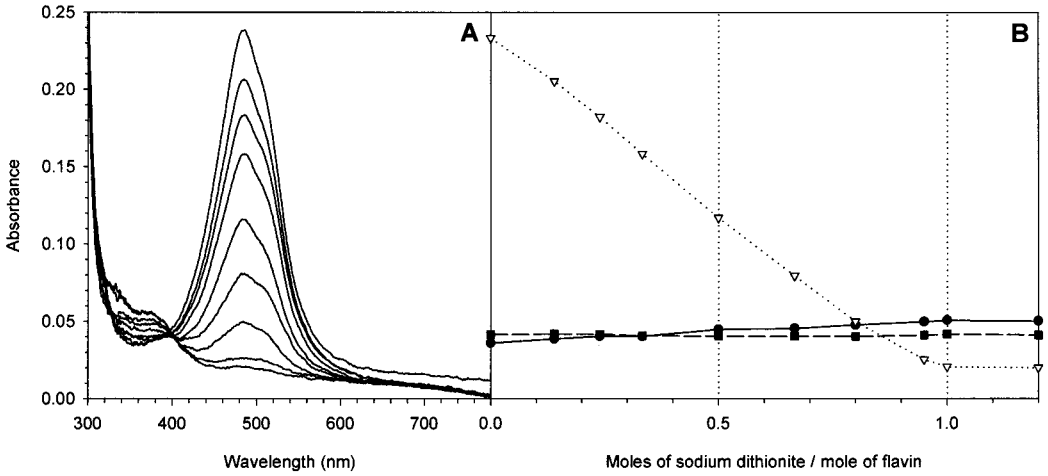

FIGURE 9: Anaerobic titration of the oxidized 8-NH_2-FMN-substituted FMN-binding domain of P450BM-3 with sodium dithionite. The 8-NH_2-FMN-substituted FMN-binding domain (7 μM) in 100 mM phosphate buffer, pH 7.0, was titrated with sodium dithionite (2 mM). Panel A represents a single titration of the protein. Panel B is a plot of absorbance changes at 380 nm (●), 400 nm (■), and 484 nm (▽) as a function of apoprotein added.

1, therefore, likely reflects oxygen leakage into the "anaerobic" titration cell.

Reduction of the 8-NH_2-FMN-substituted FMN-binding domain proceeded in one phase (Figure 9), with gradual and complete bleaching of the absorbance at 484 nm and the appearance of an absorbance band at 380 nm and an isosbestic point at 400 nm. No formation of a flavin semiquinone species was observed during anaerobic titrations of this protein with sodium dithionite. According to the stoichiometric amounts of sodium dithionite added and protein reduced, the 8-NH_2-FMN-substituted FMN-binding domain could accept 2 electron equiv during reduction.

Catalytic Activities. The ability of the flavin-substituted FMN-binding domains to carry out electron transfer to cytochrome *c* and BMP was examined in a reconstitution system consisting of the separate domains of P450BM-3. The FAD-dependent cyctochrome c reductase activities of the FMN- and 8-Cl-FMN-substituted FMN-binding domains appear to be mainly conserved and were 84 and 74% of that for the native FMN-binding domain (Table 1). The 8-NH_2-FMN-substituted FMN-binding domain was found to retain

Table 1: FAD-Binding Domain-Dependent Cytochrome *c* Reductase Activity of the Native and Flavin-Substituted FMN-Binding Domain of P450BM-3

	turnover [mol min^{-1} (mol of FMN)$^{-1}$][a]	%
native FMN-binding domain	15.5 ± 3.1	100
reconstituted FMN-binding domain	13.0 ± 2.7	84
8-Cl-FMN-substituted FMN-binding domain	11.5 ± 2.0	74
8-NH_2-FMN-substituted FMN-binding domain	4.5 ± 1.2	29

[a] The reaction mixture contained 50 mM MOPS, pH 7.5, 100 μM cytochrome *c*, and either 20 nM FAD domain, 200 nM FMN domain, or these two domains together. The reaction was initiated by the addition of 100 μM NADPH and was carried out at 30 °C. The activity, measured in the presence of either of the flavin domains, was deducted from that determined in the presence of both of them. The resulting value was considered as the FAD domain-dependent cytochrome *c* reductase activity of the FMN domain. Each value is the average of at least three independent determinations.

Table 2: Binding of FMN to Representative Flavoproteins

protein	K_d, nM	k_{on}, $M^{-1}s^{-1}$	pH[a]	ref
Old Yellow Enzyme	0.1	1×10^6	7.0	(*46*)
A. variablilis flavodoxin	0.19	2.6×10^5	7.0	(*37*)
D. vulgaris flavodoxin	0.24	7.1×10^5	7.0	(*37*)
M. elsdenii flavodoxin	0.43	3.5×10^5	7.0	(*47*, *48*)
Az. vinelandii flavodoxin	0.44	1.1×10^5	7.0	(*37*)
	5.9	2.0×10^5	7.0	(*26*)
spinach ferredoxin−$NADP^+$ reductase	3.4	1.5×10^5	7.5	(*49*)
liver NADPH-cytochrome P450 reductase	13	3.3×10^5	7.7	(*50*)
C. beijerinckii flavodoxin	18	−	7.0	(*51*)
FMN-binding domain of P450BM-3	30	1.7×10^5	7.0	present work
M. smegmatis lactate oxidase	175	1.0×10^4	7.8	(*52*)

[a] All experiments use 25−100 mM phosphate buffers unless otherwise indicated.

only approximately 30% of the cytochrome *c* reductase activity of the native enzyme.

The FMN-substituted FMN-binding domain was capable of transferring electrons to BMP in a reconstitution system consisting of the three separate domains of P450BM-3 (data not shown). As with the native FMN-binding domain, only primary metabolites, ω-1, ω-2, and ω-3 monohydroxypalmitic acids, were produced (30 and 45% conversion of palmitic acid within 10 and 30 min, respectively). In the reconstitution system with the 8-Cl-FMN-substituted FMN-binding domain, only traces of primary products were formed, where 1.8 and 3.2% of the total amount of palmitic acid were metabolized within 10 and 30 min of the reaction, respectively. No product formation was detected in the reconstitution system with 8-NH_2-FMN-substituted FMN-binding domain.

DISCUSSION

The results presented in this paper show that FMN can be reversibly removed from the FMN-binding domain of P450BM-3. The apoprotein was found to bind FMN and give a complex that has the same light absorbance and fluorescence properties, catalytic activity, and oxidation−reduction behavior as the native protein.

Table 2 compares the dissociation constants and, where available, rate constants for FMN binding to FMN-containing flavoproteins. Compared to flavodoxins, whose K_ds for complex formation of the apoprotein with FMN vary from 0.24 to 12.5 nM (*27*−*29*), the apo-FMN-binding domain of P450BM-3 appears to bind FMN less tightly (K_d = 30 nM). The weaker binding of the flavin could be a consequence of structural differences of the FMN-binding site in P450BM-3 and flavodoxins. According to the sequence alignments (*1*, *30*, *31*) and known 3-D structures of flavodoxins (*32*), the length of the peptide loop, wrapping the inner face of the isoalloxazine ring of the FMN in the FMN-binding domain, seems to be one residue shorter. The shorter length of the inner loop and the presence of two rigid prolines at the end of it could be factors that restrict the flexibility of the FMN-binding peptide.

Chemical modifications of the redox-active isoalloxazine ring of the FMN and FAD have been successfully used to probe the mechanism of action of different flavoproteins and to characterize their flavin-binding sites (*33*). We therefore decided to investigate the effect of flavin modifications on the spectral and catalytic properties of the FMN-binding domain of P450BM-3. For this purpose, 8-Cl-FMN and 8-NH_2-FMN were used, where the former represents a high-potential flavin (E_{m7} = −150 mV) and the latter is a low-potential flavin (E_{m7} = −310 mV), compared to free FMN (E_{m7} = −205 mV) (*34*). Here we report that the FMN redox center of the FMN-binding domain of P450BM-3 can be replaced with these flavin analogues, and stable, redox-active complexes can be generated with properties different from those of the native protein.

Both flavin analogues were found to form tight complexes with the apo-FMN-binding domain with affinity similar to that for native FMN. Based on the crystal structure of the BMP/FMN-binding domain complex (*20*), one would expect that substitution of the solvent-exposed 8-methyl group of FMN would have only a minimal effect on binding. This was indeed found to be the case, and the fact that the protein interacts with substituted flavins fairly indiscriminately indicates that substituted flavins may be used as powerful probes of the thermodynamic mechanism of the protein. Although based on only three points, it is interesting to note that the trend in binding constants follows the trend in redox potentials for 8-NH_2-FMN, FMN, and 8-Cl-FMN (23, 30, and 117 nM, respectively). This may actually be a result of the charge distribution within the three cofactors. Whereas the 8-NH_2 group is electron-donating and would cause a slight buildup of negative charge on the interior side of the isoalloxazine ring (with concomitant buildup of positive charge on the solvated methyl edge), the 8-Cl-withdrawing group would do just the opposite. Thus, altered interaction of the flavin dipole with the two positively charged residues on the interior side of the active site (*20*) would provide an effect qualitatively consistent with the observed trend in dissociation constants.

Structural changes have been proposed for flavoproteins exhibiting multistep kinetics as observed here for the FMN-binding domain of P450BM-3. In the *A. vinelandii* flavodoxin study mentioned previously, it was shown that the second equilibrium depends on the existence of the phosphate group of the FMN cofactor, and is not observed in riboflavin-binding studies. This fact and previously observed reversible changes in protein secondary and tertiary structure upon binding FMN as indicated in the CD spectrum caused Edmondson and Tollin (*35*) to propose that after the initial binding of the FMN cofactor to this flavodoxin the phosphate group causes a protein conformation change.

Similar CD changes occur in *C. pasteuranium*, *P. elsdenii*, *D. vulgaris*, and *R. rubrum* (*36*), so the effect was proposed to be a general property of flavodoxin−FMN interactions. The similarity of binding kinetics in P450BM-3 implies that it also extends to the highly homologous cytochrome P450 reductases. More recently in the flavodoxin literature, however, many flavodoxins have been shown to display only simple, single exponential decay of flavin fluorescence upon complex formation (*37*, *38*). Note that one study includes *A. vinelandii*, although this study only monitors kinetics over a short time frame (*37*). Complicating studies such as these is the fact that buffer composition has a major effect on flavin binding kinetics (*39*, *40*) and that flavin binding kinetics in some flavodoxins have been shown to vary with protein concentration due to protein aggregation that occurs in some

apoflavodoxins but not in the corresponding holoproteins (*40*−*42*).

One of the several arguments for a flavin−phosphate-induced protein conformation change was that previous work in Tollins' group (*43*) indicated that the phosphate group was required for "stable semiquinone formation"(*26*), with the implication that the presence of a phosphate group induced a protein conformation change that protected a formed flavin radical from external quenching agents. This would agree well with the picture of flavodoxins as one electron-transfer agents.

It has been previously shown, however, that unlike microsomal P450 reductase and flavodoxins, the FMN-binding domain of P450BM-3 and BMR do not stabilize any form of flavin semiquinone during equilibrium titrations with sodium dithionite (*6*, *17*). The FMN- and 8-NH_2-FMN-substituted FMN-binding domains also did not produce thermodynamically stable one-electron-reduced species during anaerobic titrations with sodium dithionite. On the contrary, 8-Cl-FMN substitution of the FMN-binding domain appeared to significantly perturb the redox properties of the protein. 8-Cl-FMN-binding domain was found to stabilize the red, anionic semiquinone.

Since the FAD-binding domain-dependent cytochrome *c* reductase activity of the FMN- and 8-Cl-FMN-substituted FMN-binding domains was mainly conserved (84 and 74% of that of the native protein), one can conclude that these enzymes were capable of accepting electrons from the FAD-binding domain and transferring them to cytochrome *c*. In other words, the 8-chloro substituent in the FMN was not altering the interaction with the FAD-binding domain and cytochrome *c*. The 8-NH_2-FMN substitution decreased the cytochrome *c* reductase activity of the FMN-binding domain by two-thirds. The latter result is probably a thermodynamic effect, since as stated previously the reduction potential of this analogue is −310 mV for the free form, compared to −205 mV for free FMN. The reported two-electron reduction potential of the FAD cofactor in the isolated FAD-binding domain is −303 mV (*44*), making FAD to FMN electron transfer no longer a highly energetically favorable process. Thus, it is unlikely that the analogue interferes with domain−domain interactions but rather simply has too low of a potential for electron transfer from FAD to FMN.

Strikingly, neither of the FMN analogues could reconstitute palmitic acid hydroxylase activity of the native FMN-binding domain. Traces of the primary products of palmitic acid hydroxylation were detected in the extracts from the reaction mixture containing the 8-Cl-FMN-substituted FMN-binding domain, while the 8-NH_2-substituted FMN-binding domain failed to produce any. It can be suggested that the redox potential of the high-potential flavin, 8-Cl-FMN, is being raised on binding to the apo-FMN-binding domain. Since the substrate-bound BMP is not capable of accepting electrons from reduced 8-Cl-FMN-substituted FMN-binding domain, the midpoint redox potentials for both half-reactions involving 8-Cl-FMN must be higher than −170 mV (*45*).

The ability to remove the FMN cofactor of the FMN-binding domain of P450BM-3 and replace it with analogues displaying altered redox potentials and/or chemical reactivity should prove to be a very powerful tool for examination of the mechanism of electron transfer and control of specificity in this model P450 reductase/P450 system. The possible existence of a flavin-induced conformational change in the FMN-binding domain of P450BM-3 provides initial clues into the mechanism of electron transfer from NADPH, through the FAD cofactor of the FAD-binding domain to the FMN cofactor of the FMN-binding domain and finally from the FMN cofactor to the heme in BMP. Reciprocally, interdomain protein−protein interactions would be reasonably expected to exert an influence on the FMN cofactor properties. Further studies are underway in our lab to explore this possibility by extending the techniques developed herein.

ACKNOWLEDGMENT

We thank Dr. Vincent Massey of the Department of Biological Chemistry of The University of Michigan for graciously providing the flavin analogues and advice on the analogue substitution experiments.

REFERENCES

1. Narhi, L. O., and Fulco, A. J. (1987) *J. Biol. Chem. 262*, 6683−6690.
2. Ruettinger, R. T., Wen, L. P., and Fulco, A. J. (1989) *J. Biol. Chem. 264*, 10987−10995.
3. Narhi, L. O., Wen, L. P., and Fulco, A. J. (1988) *Mol. Cell. Biochem. 79*, 63−71.
4. Li, H. Y., Darwish, K., and Poulos, T. L. (1991) *J. Biol. Chem. 266*, 11909−11914.
5. Oster, T., Boddupalli, S. S., and Peterson, J. A. (1991) *J. Biol. Chem. 266*, 22718−22725.
6. Sevrioukova, I., Truan, G., and Peterson, J. A. (1996) *Biochemistry 35*, 7528−7535.
7. Govindaraj, S., and Poulos, T. L. (1997) *J. Biol. Chem. 272*, 7915−7921.
8. Sevrioukova, I., Truan, G., and Peterson, J. A. (1997) *Arch. Biochem. Biophys. 340*, 231−238.
9. Boddupalli, S. S., Oster, T., Estabrook, R. W., and Peterson, J. A. (1992) *J. Biol. Chem. 267*, 10375−10380.
10. Porter, T. D., and Kasper, C. B. (1986) *Biochemistry 25*, 1682−1687.
11. Porter, T. D. (1991) *Trends Biochem. Sci. 16*, 154−158.
12. Smith, G. C., Tew, D. G., and Wolf, C. R. (1994) *Proc. Natl. Acad. Sci. U.S.A. 91*, 8710−8714.
13. Hodgson, A. V., and Strobel, H. W. (1996) *Arch. Biochem. Biophys. 325*, 99−106.
14. Kim, J. J. P., Wang, M., Roberts, D. L., Paschke, R., Shea, T., and Masters, B. S. S. (1996) in *Abstracts: XIth International Symposium on Microsomes and Drug Oxidations*, Los Angeles, CA.
15. Wang, M., Roberts, D. L., Paschke, R., Shea, T. M., Masters, B. S., and Kim, J. J. (1997) *Proc. Natl. Acad. Sci. U.S.A. 94*, 8411−8416.
16. Sevrioukova, I. F., and Peterson, J. A. (1995) *Biochimie 77*, 562−572.
17. Sevrioukova, I., Shaffer, C., Ballou, D. P., and Peterson, J. A. (1996) *Biochemistry 35*, 7058−7068.
18. Iyanagi, T., Makino, N., and Mason, H. S. (1974) *Biochemistry 13*, 1701−1710.
19. Iyanagi, T., Anan, F. K., Imai, Y., and Mason, H. S. (1978) *Biochemistry 17*, 2224−2230.
20. Sevrioukova, I. F., Li, H., Zhang, H., Peterson, J. A., and Poulos, T. L. (1999) *Proc. Natl. Acad. Sci. U.S.A. 96*, 1863−1868.
21. Lowry, O. H., Rosebrough, N. J., Farr, A. L., and Randall, R. J. (1951) *J. Biol. Chem. 193*, 265−275.
22. Omura, T., and Sato, R. (1964) *J. Biol. Chem. 239*, 2370−2378.
23. Whitby, L. G. (1953) *Biochem. J. 53*, 437−442.
24. Wassink, J. H., and Mayhew, S. G. (1975) *Anal. Biochem. 68*, 609−616.
25. Bradford, M. M. (1971) *Anal. Biochem. 72*, 248−254.

26. Barman, B. G., and Tollin, G. (1972) *Biochemistry 11*, 4746−4754.
27. Curley, G. P., Carr, M. C., Mayhew, S. G., and Voordouw, G. (1991) *Eur. J. Biochem. 202*, 1091−1100.
28. Mayhew, S. G. (1971) *Biochim. Biophys. Acta 235*, 289−302.
29. Dubourdieu, M., le Gall, J., and Favaudon, V. (1975) *Biochim. Biophys. Acta 376*, 519−532.
30. Ludwig, M. L., and Luschinski, C. L. (1992) in *Chemistry and Biochemistry of Flavloenzymes* (F., M., Ed.) pp 427−466, CRC Press, Boca Raton, FL.
31. Porter, T. D., and Kasper, C. B. (1985) *Proc. Natl. Acad. Sci. U.S.A. 82*, 973−977.
32. Mayhew, S. G., and Ludwig, M. L. (1975) *Enzymes (3rd Ed.) 12*, 57−118.
33. Ghisla, S., and Massey, V. (1986) *Biochem. J. 239*, 1−12.
34. Stankovich, M. T. (1991) in *Chemistry and biochemistry of flavoenzymes* (Muller, F., Ed.) pp 401−415, CRC Press, Boca Raton, FL.
35. Edmondson, D. E., and Tollin, G. (1971) *Biochemistry 10*, 124−132.
36. D'Anna, J. A., Jr., and Tollin, G. (1972) *Biochemistry 11*, 1073−1080.
37. Pueyo, J. J., Curley, G. P., and Mayhew, S. G. (1996) *Biochem. J. 313*, 855−861.
38. Gast, R., and Muller, F. (1978) *Helv. Chim. Acta 61*, 1353−1363.
39. Pueyo, J. J., Mayhew, S. G., and Voordouw, G. (1992) *Biochem. Soc. Trans. 20*, 83S.
40. Shiga, K., and Tollin, G. (1974) *Biochemistry 13*, 3268−3273.
41. Fitzgerald, M. P., Sykes, G. A., and Rogers, L. J. (1980) *Biochim. Biophys. Acta 625*, 127−132.
42. Fitzgerald, M. P., and Rogers, L. J. (1979) *Biochem. Soc. Trans. 7*, 1264−1266.
43. Edmondson, D. E., and Tollin, G. (1971) *Biochemistry 10*, 133−145.
44. Daff, S. N., Chapman, S. K., Turner, K. L., Holt, R. A., Govindaraj, S., Poulos, T. L., and Munro, A. W. (1997) *Biochemistry 36*, 13816−13823.
45. Fisher, M. T., and Sligar, S. G. (1985) *Biochemistry 24*, 6696−6701.
46. Theorell, H., and Nygaard, A. P. (1954) *Acta Chem. Scand. 8*, 1649.
47. Gast, R., Valk, B. E., Muller, F., Mayhew, S. G., and Veeger, C. (1976) *Biochim. Biophys. Acta 446*, 463−471.
48. Vervoort, J., van Berkel, W. J., Mayhew, S. G., Muller, F., Bacher, A., Nielsen, P., and LeGall, J. (1986) *Eur. J. Biochem. 161*, 749−756.
49. Zanetti, G., Cidaria, D., and Curti, B. (1982) *Eur. J. Biochem. 126*, 453−458.
50. Muller, F., and van Berkel, J. H. (1991) in *Chemistry and Biochemistry of Flavoenzymes* (Muller, F., Ed.) pp 261−274, CRC Press, Boca Raton, FL.
51. Druhan, L. J., and Swenson, R. P. (1998) *Biochemistry 37*, 9668−9678.
52. Choong, Y. S., Shepherd, M. G., and Sullivan, P. A. (1975) *Biochem. J. 145*, 37−45.

BI000255P